This version is available at https://strathprints.strath.ac.uk/62559/

CrossMark

Hybrid effects in thin ply carbon/glass unidirectional laminates: Accurate experimental determination and prediction

M.R. Wisnom [a,*], G. Czél [b,a], Y. Swolfs [c], M. Jalalvand [a], L. Gorbatikh [c], I. Verpoest [c]

[a] Advanced Composites Centre for Innovation and Science, University of Bristol, Queen's Building, BS8 1TR Bristol, United Kingdom
[b] MTA–BME Research Group for Composite Science and Technology, Budapest University of Technology and Economics, Műegyetem rkp. 3, H-1111 Budapest, Hungary
[c] Department of Materials Engineering, KU Leuven, Kasteelpark Arenberg 44 bus 2450, B-3001 Leuven, Belgium

ABSTRACT

Experimental results are presented which allow the hybrid effect to be evaluated accurately for thin ply carbon/epoxy–glass/epoxy interlayer hybrid composites. It is shown that there is an enhancement in strain at failure of up to 20% for very thin plies, but no significant effect for thicker plies. Hybrid specimens with thick carbon plies can therefore be used to measure the reference carbon/epoxy failure strain. The latter is significantly higher than the strain from all-carbon specimens in which there is an effect due to stress concentrations at the load introduction. Models are presented which illustrate the mechanisms responsible for the hybrid effect due to the constraint on failure at both the fibre and ply level. These results give a good understanding of how variability in the carbon fibre strengths can translate into hybrid effects in composite laminates.

© 2016 The Authors. Published by Elsevier Ltd. This is an open access article under the CC BY license (http://creativecommons.org/licenses/by/4.0/).

1. Introduction

Ever since Hayashi reported in 1972 that the failure strain of the carbon fibre layers in a carbon/glass hybrid composite was 40% higher than in the reference carbon fibre composite [1] there has been much interest and controversy over the so called hybrid effect. In a recent review Swolfs et al. concluded that the effect for tensile failure strain is well established, with a typical range of 10–50% for traditional hybrid composites such as carbon/glass [2]. The basic mechanisms responsible for the hybrid effect were reviewed, with the most significant considered to be thermal residual stresses, altered failure development due to statistical effects on formation of clusters of fibre breaks and dynamic stress concentrations. Phillips [3] documented the scientific discussions shortly after the discovery of the hybrid effect. A number of other researchers have made notable contributions [4–8], with a gradual improvement in the understanding and predictive modelling of the hybrid effect in the seventies and eighties.

However, there are many difficulties in measuring the baseline tensile failure strain of a high strength unidirectional (UD) composite against which the strain at failure of the hybrid is compared to determine the hybrid effect. The strain to failure of the baseline low elongation material is referred to here as the reference strain to failure, and it may be significantly underestimated due to issues

with the test methods such as stress concentrations at the load introduction regions. These effects may be responsible for some of the variability and high values claimed in certain cases for the hybrid effect. In this paper a new method is used to deduce the reference strain to failure of the low strain component of the hybrid and it is demonstrated that this method gives substantially higher and more realistic failure strains than conventional approaches.

Tests reported here with thin ply carbon/glass laminates enable the hybrid effect to be accurately determined. It is demonstrated that there is an enhancement to the failure initiation strain, the point when the carbon starts to fracture, but only when the carbon plies are very thin. In addition there is a second strength enhancement mechanism that arises if multiple fractures of the carbon can occur stably, and in this case the strength is effectively the point where a sufficient number of fractures have occurred to significantly reduce the stiffness of the hybrid rather than the first carbon fracture. This illustrates that the hybrid effect is intimately linked to variability of strength, confirming the view of Manders that "the hybrid effect arises from a failure to realise the full potential strength of the fibres in all-carbon fibre composites, rather than from an enhancement of their strength in the hybrids" [9].

This paper describes the accurate determination of the baseline carbon fibre strain to failure and then quantifies the magnitude of the hybrid effect for initiation of failure in carbon/glass hybrids with different carbon ply thicknesses. The additional hybrid effect due to multiple fractures is then demonstrated and quantified.

Table 1
Fibre properties of the applied UD prepregs (based on manufacturer's data).

Fibre type	Manufacturer	Elastic modulus (GPa)	Strain to failure (%)	Tensile strength (GPa)	Density (g/cm^3)
Pyrofil TR30 carbon	Mitsubishi rayon	234	1.9	4.4	1.79
FliteStrand S ZT S-glass	Owens corning	88	5.5	4.8–5.1	2.45

Table 2
Cured ply properties of the applied UD prepregs.

Prepreg material	Fibre mass per unit area (g/m^2) (CV (%))[a]	Cured ply thickness (mm)	Fibre volume fraction (%)	Initial elastic modulus (GPa) (CV (%))	Strain to failure[c] (%) (CV (%))
TR30 carbon/epoxy	21.2 (4.0) [16]	0.029 [16]	41 [16]	101.7 (2.75) [15]	1.50 (7.5) [15]
S-glass/913 epoxy	190[b]	0.155[b]	50[b]	45.7 (3.0) [17]	3.98 (1.1) [17]

Values with references were determined experimentally.
[a] Coefficient of variation.
[b] Based on manufacturer's data.
[c] From conventional tensile tests.

Models for predicting both effects are described, and it is shown that they are able to capture and explain the observed phenomena.

2. Accurate determination of baseline strain to failure

Standard straight-sided specimens tend to underestimate the true ultimate strength of unidirectional composite materials. Stress concentrations arise where the load is introduced [10], but with very careful tapering of the specimens by chamfering plies through the thickness, gauge section failures can be achieved with significantly higher strains to failure [11,12]. In most reported hybrid composite studies, there were no such efforts to avoid tab failure, and so premature failure and decreased strains may have been recorded as the baseline. In this paper a different approach is adopted based on [13] to determine the baseline carbon fibre strength from carbon plies sandwiched between glass plies. The surface glass protects the interior carbon, and finite element analysis has revealed that there are no stress concentrations in the carbon layer, but only in the glass layer. This promotes carbon layer failure initiation in the gauge section, as has been verified experimentally [13]. Crucially, it will be shown later that when the carbon plies are not too thin, there is no significant strain enhancement in the presence of glass, and the tests can provide accurate values for the baseline strength of the carbon fibre composite.

The different failure mechanisms in carbon/glass laminates have been studied, and found to depend on the ratio of carbon to glass thickness and also the absolute thickness of the carbon [14]. With the right thicknesses it has been demonstrated that following first fracture of the carbon, the glass does not fail, but delamination occurs between the carbon and glass. This requires that the proportion of carbon is lower than the limit for premature glass failure and the absolute thickness is high enough to generate delamination rather than ply fragmentation. Delamination can be observed visually due to the translucence of the glass. The specimens are initially black due to the carbon, but after delamination, light is reflected from the interface, and the specimens appear yellow. It can also be seen clearly where failure has occurred, which is typically in the gauge section. This delaminating hybrid specimen is the method used here to determine the baseline strength of the carbon.

The basic properties of the fibres and prepregs applied are summarised in Tables 1 and 2. Specimens were vacuum bagged and cured in an autoclave at 125 °C for one hour. Although the resins of the glass and carbon fibre prepregs were different, the recommended cure cycles were the same for both manufacturers, and
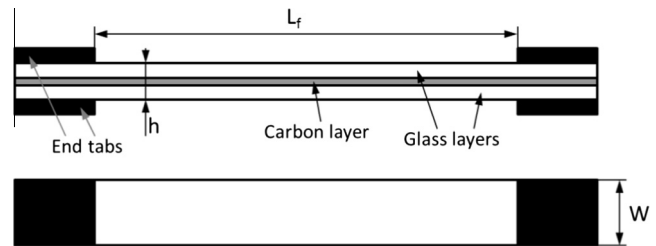

Fig. 1. Schematic of an interlayer hybrid composite specimen.

there were no issues with resin incompatibility. Specimens were well consolidated, although the volume fractions were relatively low. Nominal thicknesses of each specimen type (based on the ply thickness data of Table 2) were used for data evaluation to compensate for the small variation (less than 3% CV) in thickness within the specimen series which is attributed to the variation in resin content.

The tensile testing of the 16 ply all carbon (16C) specimens is described in [15]. The specimen size was 180/100/10 mm overall length/free length/width. The interlayer hybrid specimens had a three layer sandwich structure as shown in Fig. 1, with thin (0.029 mm) carbon plies between standard thickness (0.155 mm) glass plies. The nominal sizes were 240/160/20 mm overall length/free length/width respectively. Ideally the same dimensions would have been used for both specimen types. The volume of the carbon in the hybrid specimens is 60% and 80% of that in the all carbon ones. The effect of such differences in stressed volume is considered in Section 3, and shown to be relatively small. Unchamfered 40 mm long cross-ply S-glass/epoxy end-tabs were used on all specimens.

The experimental results of the thin-ply UD hybrid composites analysed here were generated as part of a wider experimental programme, reported in [18] with emphasis on their pseudo-ductility. Testing of the parallel edge specimens was executed under uniaxial tensile loading and displacement control using crosshead speeds of 1 mm/min for the all carbon specimens and 2 mm/min for the longer, lower modulus hybrid specimens, giving similar times to failure. A computer controlled Instron 8801 universal hydraulic test machine with a regularly calibrated 100 kN Instron Dynacell load cell and wedge type hydraulic grips was used for the tensile tests. Strains were measured using an Imetrum videogauge system, with a nominal gauge length of 130–140 mm. The test results are summarised in Table 3. They are very consistent, with low coefficients of variation of around only 2%.

Table 3
Tested baseline configurations and results (specimen type designation: C- thin carbon and SG- standard thickness S-glass ply with the numbers corresponding to the number of plies).

Specimen type	No. of spec. tested	Nominal thickness (mm)	Carbon/epoxy failure strain at load-drop (%) (CV (%))	Initial compressive thermal strain in carbon (%)	Corrected carbon failure strain (%)
16C	10 [15]	0.464 [15]	1.500 (7.5) [15]	–	–
2SG/4C/2SG	4	0.736	1.900 (1.5)	−0.023	1.877
1SG/3C/1SG	5	0.397	1.859 (2.1)	−0.020	1.839
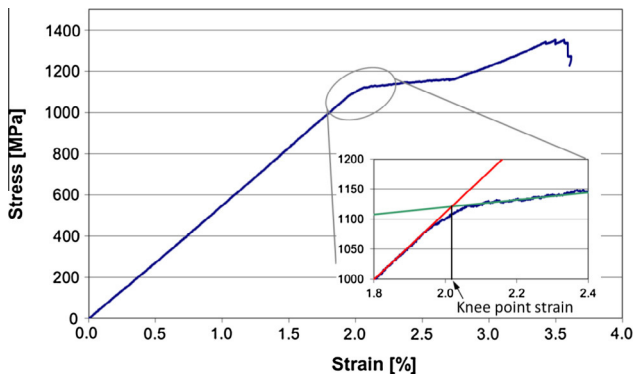
Fig. 2. Typical non-linear response of (1SG/2C/1SG) laminate.

Fig. 3. Dependency of carbon layer failure strain on the thickness showing a hybrid effect.

The average strain at failure as measured at the point of the load drop when unstable delamination occurs is 1.900% and 1.859% for the cases with 4 and 3 carbon plies. These specimens behaved similarly and the difference between them is not statistically significant. There is however a small effect of thermal residual stresses, which can be corrected based on the measured fibre direction moduli of 45.7 GPa and 101.7 GPa and typical expansion coefficients of $3.85 \times 10^{-6}\ K^{-1}$ and $0.67 \times 10^{-6}\ K^{-1}$ for the glass and carbon plies respectively, with 100 °C difference between the cure and room temperatures. This gives small residual strains of −0.023% and −0.020% in the carbon layers. The effect of resin shrinkage would be negligible, as it normally contributes very little – less than 5% of the residual stress in one study on cross-ply laminates [19]. An even lower effect would be expected in unidirectional hybrids where stresses are driven by the difference in fibre expansion coefficients rather than by matrix contraction. The corrected elastic tensile strains at failure for the two cases are therefore 1.877% and 1.839%. The mean value of 1.858% is believed to be representative of the true ultimate strain of the carbon fibre plies since it corresponds to visually observed catastrophic failure away from any stress concentrations. This value is not significantly influenced by a hybrid effect, as shown experimentally in Section 3 and by modelling in Section 5. It also corresponds closely to the 1.9% fibre strain quoted by the manufacturer on the datasheet.

On the other hand the experimental value of 1.50% from the all carbon specimens is clearly too low, as will be shown later, and is believed to have been affected by premature failure due to the specimen design and gripping conditions. However, if this value had been used as a baseline, following the approach used in many other previous studies, then it might have been concluded that

there was a hybrid effect of about 24% in these cases with three or four carbon plies.

3. Accurate measurement of hybrid effect and influence of ply thickness

Two further series of tests on hybrid laminates similar to those described in Section 2 were carried out but with thinner carbon layers. The reduced energy release rate due to the thinner plies meant that when the carbon fractured, complete delamination of the whole specimen did not occur. The materials were the same standard thickness S-glass/epoxy and thin carbon/epoxy, with lay-ups (1SG/1C/1SG) and (1SG/2C/1SG).

These thin ply hybrids developed progressive multiple fragmentations of the carbon, leading to a pseudo-ductile stress–strain response with a plateau, analogous to yielding in metals, as shown for a typical specimen in Fig. 2. The failure initiation strains of the carbon were taken at the knee points, which can be easily established from the intersection of straight lines fitted to the elastic and plateau regions, as shown in the inset to Fig. 2. In fact there is a small amount of non-linearity before this point, which will be considered in Section 4.

The failure strains of the single and double carbon plies are given in Table 4. Taking account of the calculated initial strains due to thermal residual stresses gives corrected elastic tensile strains at failure of 2.227% and 2.004% respectively. Fig. 3 reveals the comparison of results against the strain at failure established

Table 4
Tested thin carbon layer configurations and results.

Specimen type	No. of spec. tested	Nominal thickness (mm)	Knee point strain (%) (CV (%))	Initial compressive thermal strain in carbon layer (%)	Knee point strain corrected with thermal strain (%)
1SG/1C/1SG	5	0.339	2.253 (1.4)	−0.026	2.227
1SG/2C/1SG	5	0.368	2.027 (1.6)	−0.023	2.004

from the previous tests where delamination occurred after first carbon layer failure. The strain at failure of the single carbon ply is 11.1% higher than that of the double ply, which in turn is a further 7.9% higher than the average of the cases with 3 and 4 plies that delaminated. This effect cannot be explained by residual stresses since the absolute increase in residual strain in the single compared with the double carbon ply case is only 0.003%. Another notable point is the low coefficients of variation of less than 2% in the knee point strains.

It is well known that there is a size effect in tensile strength of carbon fibres due to the higher probability of finding a cluster of weaker fibres in a larger volume of material [20]. The single ply has half the volume of the double ply case, and might therefore be expected to have a higher strain at failure due to the statistical size effect. However the magnitude of this effect is relatively small. The Weibull modulus of the carbon fibre/epoxy material is not known, but in a previous study of tensile tests with IM7 carbon fibres, a modulus of 41 was determined for the composite from the reduction in strength of scaled specimens with increasing size [21]. For a volume ratio of 2, this would lead to a relative enhancement of strain of 1.7%, small compared with the 11.1% observed experimentally. Even if the Weibull modulus of the carbon ply is lower than 41, it cannot explain the much higher strain at failure of the single ply case.

The substantial increase in strain for the single carbon ply case is believed to be caused by the restraint from the adjacent glass plies which inhibits the formation of clusters of carbon fibre breaks, as discussed in Section 5. This constitutes a substantial hybrid effect of 19.8%, due to the delay in failure of the carbon fibres. The smaller increase in strain at failure for the two ply case represents a hybrid effect of 7.9%, but beyond this thickness there does not appear to be any further effect, given the similar results with 3 and 4 plies. This justifies the use of the thicker specimens to establish the baseline reference strength.

4. Hybrid effects related to initiation and multiple fractures

In the previous section, the failure strains of the carbon layers were based on the knee in the stress–strain response. However, careful examination of the tests revealed that first failure initiation in the carbon layer actually occurred earlier. The point of first fracture of the carbon layer was established visually from studying the videos of each specimen taken with the strain measurement system. The carbon layer cracks could be detected because of the associated delamination and translucency of the glass layers, and the strains were determined from the video extensometer readings using the test time to match the videos to the strains. These results are summarised in Table 5, with the corrections for thermal residual stresses given above included.

The strain at the knee points is higher than at failure initiation by an additional 0.060% for the single and 0.041% for the double carbon ply case. Although these differences are relatively small, they are consistent from specimen to specimen, and the coefficients of variation are low.
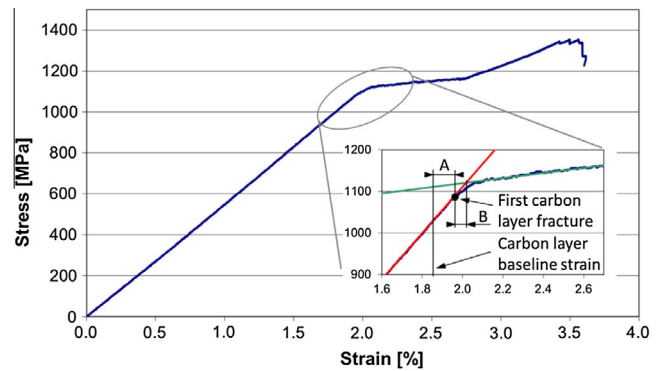

Fig. 4. Two components of the hybrid effect: delay in the initial cluster formation (A) and additional element due to established multiple fragmentation (B).

This indicates that the hybrid effect can be split into two components, the delay in initiation due to the constraint on cluster formation, and an additional element corresponding to multiple fragmentation. This arises from the fact that the knee point marking the effective strength of the carbon ply requires sufficient fractures in the carbon ply to reduce the modulus rather than corresponding to the formation of the very first critical cluster. These two components are displayed as A and B in Fig. 4 and the hybrid effects are summarised in Table 6. The hybrid effects were calculated relative to the average failure strain of the three and four carbon ply hybrids, which was 1.858%. For the single ply case the hybrid effect is 16.6% based on the initiation of failure, with a further 3.2% based on multiple fragmentation. For the two ply case the corresponding values of the hybrid effect are 5.7% for initiation and a further 2.2% at fragmentation.

5. Modelling the hybrid effect

The mechanism of the hybrid effect on initiation due to the constraint on cluster formation can be illustrated using the statistical strength model of Swolfs et al. [22–24]. This captures the distribution of individual fibre strengths together with the stress transfer and associated stress concentrations at the fibre breaks. The additional effect due to multiple fragmentation within the plies can be illustrated using the ply level finite element model of Jalalvand et al. [14] which considers the distribution of strength for the whole carbon ply, and stress transfer at the ply rather than individual fibre level.

5.1. Increase in failure initiation strain

The four tested lay-ups of carbon/S-glass hybrids are analysed in this section. These cases are labelled based on the number of carbon fibre plies in the middle, ranging from "1 carbon ply hybrid" to "4 carbon ply hybrid".

Very local load sharing and hexagonal packing were assumed, meaning that the load from a broken fibre is shed only to its 6 nearest neighbours. While the experimental V_f is different in the carbon (41%) and glass (51%) layers, such a difference in V_f is difficult to work with in a hexagonal packing. These different fractions would cause changes in the fibre spacing at the interface between dissimilar layers, and would be expected to have a negligible influence on the outcome of the model. Therefore, an overall volume fraction of 50% was chosen.

The carbon fibre was assumed to be transversely isotropic with a longitudinal fibre stiffness of 234 GPa. The other elastic constants of the fibre were the same as in Swolfs et al. [24,25], whereas the coefficients of thermal expansions were already mentioned in Sec-

Table 5
Summary of measured carbon layer failure strains, corrected for residual stresses.

Layup	Strain at first carbon layer fracture [Absolute %] (CV (%))	Strain at knee point [Absolute %] (CV (%))
1SG/1C/1SG	2.166 (2.5)	2.227 (1.4)
1SG/2C/1SG	1.963 (2.3)	2.004 (1.6)
1SG/3C/1SG	1.839 (2.1)	–
2SG/4C/2SG	1.877 (1.5)	–

Table 6
Hybrid effects for initiation and fragmentation (strains corrected for residual stresses).

Layup	Strain at first carbon layer fracture [Absolute %] (CV (%))	Strain at knee point (start of fragmentation) [Absolute %] (CV (%))	Initiation hybrid effect [Relative %] (A)	Fragmentation hybrid effect [Relative %] (B)	Total hybrid effect [Relative %] (A + B)
1SG/1C/1SG	2.166 (2.5)	2.227 (1.4)	16.6	3.2	19.8
1SG/2C/1SG	1.963 (2.3)	2.004 (1.6)	5.7	2.2	7.9
Baseline – average of 3 and 4 carbon ply delaminating hybrids	1.858	–			

Table 7
Parameters used in modelling failure initiation.

Property	Value	Source
Carbon fibre		
Longitudinal elastic modulus	234 GPa	Data sheet
Weibull modulus	5	Typical value [28]
Reference gauge length	10 mm	Chosen value
Weibull scale parameter	3029 MPa	Fitted
Ineffective length	101 μm	Predicted by FE model
S-glass		
Elastic modulus	88 GPa	Data sheet
Poisson's ratio	0.22	Typical value [28]
Weibull modulus	4	Chosen value
Reference gauge length	50 mm	Chosen value
Weibull scale parameter	1520 MPa	Chosen value
Ineffective length	53 μm	Predicted by FE model
Matrix		
Elastic modulus	3.4 GPa	Data sheet
Poisson's ratio	0.40	Typical value [28]
Model		
Overall fibre volume fraction	50%	Based on actual V_f
Layer thickness	24 μm, 57 μm, 90 μm and 122 μm (1, 2, 3 and 4 carbon ply hybrid)	Chosen to be close to experiments
Model width	2 mm	Chosen value
Model length	10 mm	Chosen value
Total number of fibres	From 2337 to 4463	Results from width, layer thickness and V_f
Number of simulations/configuration	200	Chosen value

tion 2. The S-glass fibre was assumed to be isotropic with a longitudinal stiffness of 88 GPa and a Poisson's ratio of 0.22. The matrix was assumed to be isotropic, well-bonded and linear elastic with a stiffness of 3.4 GPa and a Poisson's ratio of 0.4. Table 7 summarises the values used and where they came from. A FE model with hexagonal packing and 50% fibre volume fraction was used to calculate the ineffective length [25,27]. This is defined here as the length over which the stress in a broken fibre is less than 90% of the nominal stress [26]. The value was 101 μm and 53 μm for the carbon and glass fibre, respectively. Combining these values with the assumptions of a linear stress recovery profile and very local load sharing yields the entire stress redistribution around a fibre break.

Since the layer thickness is an important parameter in the hybrid effect, simply using the manufacturer's data sheet was insufficiently accurate. Optical microscopy images were hence used to determine the most appropriate layer thickness to model. Accurately measuring the layer thickness in the 1 carbon ply hybrid is difficult as the boundary between the layers is not clearly defined. Therefore, measurements were performed on hybrid composites with the number of carbon fibre plies varying from 1 to 4, giving an average layer thickness of 29 μm. In a hexagonal packing with a V_f of 50%, this corresponds to a layer of about three fibres thick. Similarly, the average layer thickness of the glass fibre plies was determined to be 155 μm.

The variation in layer thickness leads to a change in the fibre dispersion, i.e. the fineness or degree of mixing of the constituents. This variation needs to be taken into account, as it is known to have a significant influence on the hybrid effect for initial failure strain [22,2]. Therefore, the layer thickness of the 1 carbon ply hybrid was varied between 1 and 5 fibres thick (see Fig. 5a). The number of fibres over the thickness was always an odd number. The thickness of the 2, 3 and 4 carbon ply hybrid was randomly varied between 5–9, 9–13 and 13–17 fibres respectively. This gave averages of 3, 7, 11 and 15 fibres per layer, with thicknesses of 24 μm, 57 μm, 90 μm and 122 μm for the 1, 2, 3 and 4 carbon ply hybrid, respectively.

The glass fibre layers above and below the carbon layer were modelled to be at least three fibres thick, all along the width of the model. The glass layers are thicker in reality, but their thickness does not affect the modelling predictions. This was confirmed by modelling thicker glass fibre layers, which had no influence on the predicted failure strains. This is mainly due to the very local load sharing assumption, which causes only stress concentrations on the 6 nearest neighbours. The thickness of the glass fibre layer would however have a small influence on the thermal residual stresses, but these were not taken into account in the model, and were subtracted from the experimental results.

Boundary fibres were added to make it more representative of larger sample sizes [24]. These fibres have the same properties as the other fibres, but are not allowed to break. Their absence could make a small difference at the left and right edges of the model (see Fig. 5). The boundary fibres on the top and bottom, however, do not make a difference as the critical cluster will not develop in the glass fibre layers. The modelled width was 2 mm, while the length was 10 mm. The number of fibres ranged from 2337
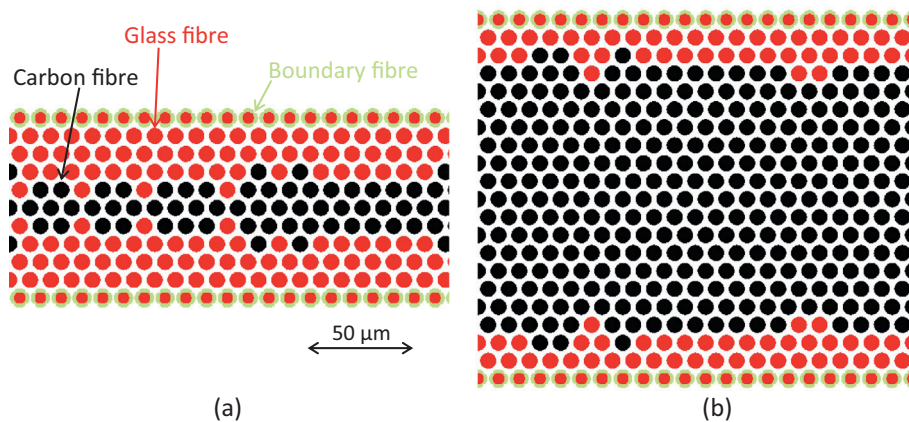
Fig. 5. Modelled geometry of the carbon/glass hybrid composites: (a) 1 carbon ply hybrid, and (b) 4 carbon ply hybrid. The width corresponds to 200 μm out of the 2 mm total width modelled.

for the 1 carbon ply hybrid to 4463 for the 4 carbon ply hybrid. Each model contained close to 1700 glass fibres, as the glass fibre layers always had the same thickness (see Fig. 5).

The Weibull distributions for both fibre types are unknown. Therefore, the following strategy was used to set up the parameters of a unimodal Weibull distribution. The carbon fibre Weibull modulus m was set to 5, which is a reasonable value for this carbon fibre type [29,30]. The gauge length L_0 was set to 10 mm, which corresponds to the actual length of the model. The Weibull scale parameter σ_0 was chosen in such a way that the predicted failure strain of the 4 carbon ply hybrid corresponded to the experimental value of 1.858%. By setting σ_0 to 3029 MPa, a failure strain of the carbon fibre plies in the 4 carbon ply hybrid of 1.856 ± 0.043% was achieved. After correcting for thermal residual stresses, this becomes 1.877 ± 0.043%. The Weibull modulus of the S-glass fibres was set to 4, as that is a reasonable value for glass fibres [31]. σ_0 and L_0 were set to 1520 MPa and 50 mm respectively to yield a reasonable failure strain of 3.9%.

A total of 200 simulations was performed for every configuration. Failure of the carbon fibre layer was detected as an exponential and unstable increase in the number of fibre breaks on successive iterations within one strain increment. This corresponds to the propagation of a critical cluster in the carbon fibre layer. The failure strain of the reference all-carbon and all-glass composites was determined using a model with the same dimensions as the 4 carbon ply hybrid (see Fig. 5b). By using boundary fibres, the exact size of these reference composites will only have minor influence on their predicted failure strain [24]. Thermal residual stresses were not added to the predicted values, although this is in principle possible. This ensures consistency with the experimental results, from which the thermal residual strains were subtracted (see Table 6).

The hybrid effect was calculated as the relative failure strain increase compared to the all-carbon fibre reference composite. The modelled failure strain of 1.836 ± 0.04% for the all-carbon composite was used as the reference value. This is slightly lower than the failure strain of the four carbon ply hybrid in the model, which was 1.856 ± 0.043%, suggesting that the 3 and 4 ply carbon hybrids may still include a very small hybrid effect. The experimental values for comparison were taken from the results presented earlier for the visual determination of the initial failure, after correction for the thermal residual stresses (see Table 6).

Fig. 6 reveals an increase in the predicted failure strain with decreasing number of carbon fibre plies. As described in detail in Swolfs et al. [22], this can be attributed to the increasing restrictions on forming clusters of fibre breaks.

There is a reasonable agreement between the model predictions and experiments. For the 1 ply carbon hybrid, the model underestimated the hybrid effect: 11.9% compared to 16.6% in the experiments based on initiation, as presented in Section 4. For the 2 carbon ply case the predicted hybrid effect is 3.3% compared to 5.7% in the experiments. The differences may be attributed to:

- *Dynamic effects:* this may further increase the hybrid effect, but its relative importance is unclear from the literature [2,32].
- *Uncertainties in the input data:* the Weibull modulus is known to be crucial for the hybrid effect [2], but is also very difficult to measure [24]. A smaller Weibull modulus would lead to larger hybrid effects in the model, and bring the modelling results closer to the experimental values.
- *Possible size scaling effects:* the model is significantly smaller than the actual tensile samples. The effect of size scaling on the hybrid effect has not yet been investigated in the literature.

Another key conclusion is that the 4 carbon ply hybrid has nearly the same failure strain as the carbon fibre reference composite. This means that carbon fibre plies with a thickness above 100 μm will have a negligible hybrid effect. Sandwiching carbon
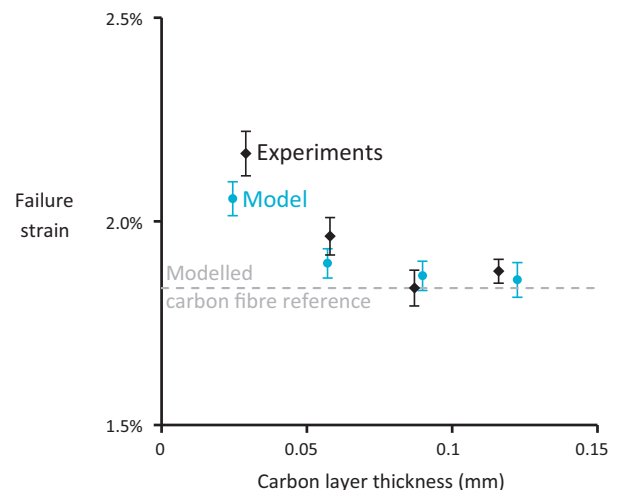

Fig. 6. Comparison between model failure strain predictions and experimental results as a function of the carbon fibre layer thickness. The error bars indicate the standard deviations. Residual stresses were not taken into account in the model, and were subtracted from the experimental results.

fibre plies in between glass fibre plies is therefore a reliable method for measuring the carbon fibre composite failure strain.

5.2. Higher carbon layer failure strain at the start of the fragmentation process

The effect of multiple fragmentation in the carbon ply is analysed with the approach proposed by Jalavand et al. [14]. This method has been used to study the effect of laminate configuration on UD hybrid tensile response and was able to accurately predict the damage processes of different UD hybrid specimens. A finite element model at the ply level is used with cohesive elements to represent interfacial failure between plies, and multiple cohesive elements embedded within the carbon plies normal to the tensile load to represent their statistical strength distribution. An identical strength distribution for the carbon layer has been used in all different hybrid laminates and the different damage developments were predicted accurately. The details of the model can be found in [14,33].

The same modelling approach was applied to predict fragmentation growth and its effect on the stress–strain curve of the 1SG/1C/1SG and 1SG/2C/1SG laminates. The modulus and ply-thickness of the S-glass/epoxy and carbon/epoxy layers were chosen according to Table 2. The Weibull modulus is not known and so the same random distribution with $m = 41$, as in Fig. 4 of [14], was applied to simulate the strength variability of the TR30 carbon/epoxy layer. The weakest point from the finite number of values in the strength distribution has a 1.92% failure strain, which is based on the carbon layer fracture of the 2EG/3C/2EG laminate (EG stands for E-glass) presented in Table 6 of [16]. This failure strain is only 0.02% higher than that of 2SG/4C/2SG as presented in Table 3 and therefore, using the same strength distribution as in [14] is plausible. Thermal residual strains were not taken into account, which is acceptable because the difference in strains for the 1SG/1C/1SG and 1SG/2C/1SG laminates is only 0.002% according to Table 3. The first failure in the finite element analysis occurs at the same overall extension in both 1SG/1C/1SG and 1SG/2C/1SG laminates since this model does not account for the hybrid effect on initiation. But the subsequently predicted fragmentation rate which determines the stress–strain curve of each laminate will be different. This initial failure strain is slightly different from the 1.86% failure strain of the laminates with 3 and 4 layers of carbon presented earlier. But there was no data available on the strength variability of this prepreg, and therefore the same strength and Weibull modulus already used for the analysis of E-glass/TR30 carbon hybrid laminates [14] as given above were employed here. The model simulates the full non-linear response of the hybrid, giving similar curves to the ones obtained experimentally. The knee point on the stress–strain response can be established by fitting lines to the data in exactly the same way as in Fig. 2.

For the case with a single ply, the first carbon fracture at 1.92% does not produce a significant change in stiffness, and the knee in the stress–strain curve is delayed until a strain of 2.04%, as shown in Fig. 7a. The reason for such delay is that the change in slope corresponds to the point at which multiple fibre fractures build up throughout the whole laminate rather than just the very first failure. However, for the case with 2 carbon plies, the knee is at 1.97%, fairly close to the first initiation of failure at a strain of 1.92%. Carbon layer fractures have a more pronounced effect on the average stress–strain curve of this hybrid laminate due to the higher contribution of the thicker carbon layer to the overall stiffness of the laminate, and the lower number of fractures required to establish the fragmentation process since the critical length of the ply increases with ply thickness. The model shows that the process zone around the tip of the carbon layer fragments in the double

carbon ply is twice as long as for the single ply case and therefore, the number and rate of crack formation are lower in the thicker carbon case.

The development of carbon layer fragmentation and associated translaminar crack density growth is also shown in Fig. 7(a) and (b) for both specimens. The initial fractures do not have much effect on the stress–strain curve, and there is a significant change in slope only when a regular process of steady fragmentation is established. The maximum predicted crack density of the 1SG/1C/1SG specimen is 1.16 mm^{-1} while it is only 0.33 mm^{-1} (3.5 times less) for the 1SG/2C/1SG laminate because of the greater ply-level critical length and local delaminations in the thicker laminate. This means that the number of cracks required to achieve saturation in the 1SG/1C/1SG sample is significantly larger than in the 2-ply case. The crack density growth has a small rise at the very beginning which is distinct from the main fragmentation process initiating at 2.04%. Therefore, the apparent slope change is not obvious until this strain value. Since the ratio of carbon in the 1SG/2C/1SG specimen type is much higher than that for the 1SG/1C/1SG type, the effect of each carbon layer fragmentation event is accompanied by more noticeable stress fluctuations on the overall stress–strain curve. As a result, the intersection of the initial slope and secondary average lines is at 1.97%, much closer to the first fibre failure strain. These results are aligned with the experimental results in Table 6. They can be compared by taking the difference between the knee point and the first carbon layer fracture, which should not depend on the initiation hybrid effect. The difference in the model
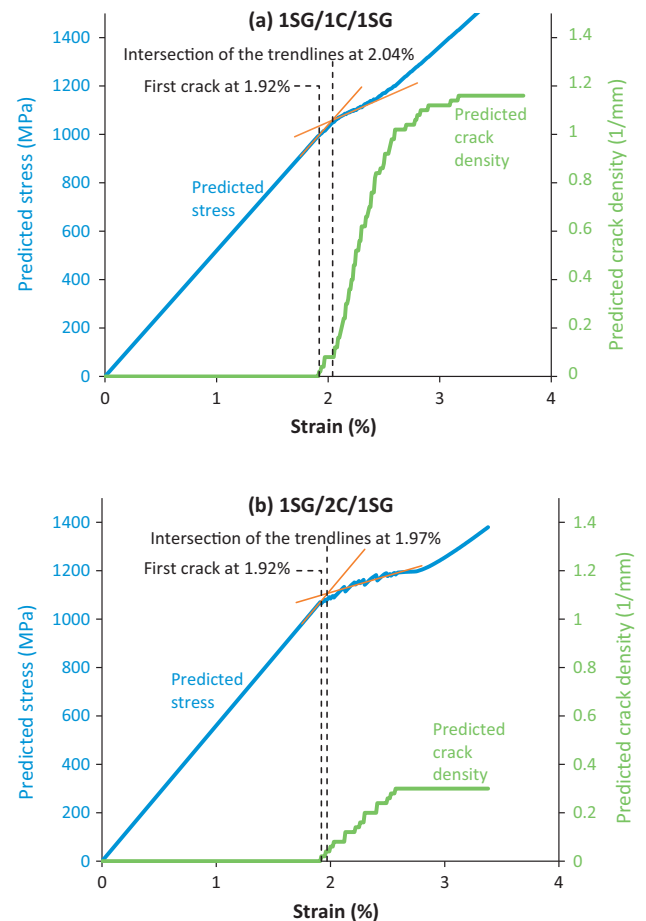

Fig. 7. Predicted stress–strain and crack density curves for different carbon ply thicknesses showing the delay in establishing ply fragmentation in the thinner ply case.

Table 8
Summary of strains at different stages of failure of the carbon ply (corrected for residual stresses).

Layup	Measured strain at first carbon layer fracture	Measured strain at first knee (start of fragmentation)	Calculated strain in carbon layer at second knee (end of fragmentation)
	[Absolute %] (CV (%))	[Absolute %] (CV (%))	[Absolute %] (CV (%))
1SG/1C/1SG	2.166 (2.5)	2.227 (1.4)	2.352 (2.2)
1SG/2C/1SG	1.963 (2.3)	2.004 (1.6)	2.108 (0.4)
Baseline – average of 3 and 4 carbon ply delaminating hybrids	1.858	–	–

is 6.2% and 2.6% in relative terms for the single and double carbon layers respectively, compared with equivalent experimental values of 3.2% and 2.2%. The values are higher than measured, but the model correctly predicts the larger effect in the specimen with one carbon layer and explains the mechanism in terms of the larger number of cracks required to have an effect on the apparent stress–strain curve.

Note that the fracture initiation strain is the same in both cases as this is an input parameter to the model and the effect of ply thickness on the initiation hybrid effect cannot be predicted with this approach. On the other hand the model presented in Section 5.1 is able to predict the difference in initiation strains, but cannot represent the ply fragmentation process. The models are therefore complementary to each other in explaining the hybrid effects observed experimentally.

5.3. Further increase in carbon layer failure strain during fragmentation

An analytical model of the fragmentation process was also established [34] which revealed that for a fixed carbon ply failure strain, fragmentation occurs at constant stress, giving a flat plateau. However the stress level required for multiple cracking increases during the fragmentation process due to the statistical distribution of carbon fibre strengths. As a result, the stress slightly rises along the plateau until the ply fragmentation becomes saturated. At this point, there is a second knee as the stress in the glass starts to rise with the load contribution of the carbon layer remaining constant due to the inability to transfer any further load across the interface. At the second knee point, the strain varies along the specimen both in the carbon and glass layers and the average strain in the carbon is no longer equal to the external extension. The analytical model [34] allows to relate the strength of the carbon at the fragmentation saturation point, S_C, to the overall laminate-level stress, σ, according to Eq. (1):

$$\sigma = \frac{S_C}{E_C} \frac{E_G t_G + E_C t_C}{t_C + t_G},$$ (1)

where E and t are the modulus and thickness of the glass/epoxy (*G*) and carbon/epoxy (*C*) layers.

To find the strain at the point of the last fracture in the carbon layer, ϵ_C, which corresponds to fragmentation saturation, Eq. (1) is rewritten as :

$$\epsilon_C = \sigma \frac{t_C + t_G}{E_G t_G + E_C t_C}$$ (2)

This is the maximum value in the middle of the fragments of the carbon layer when saturation is complete, i.e. at a crack density of 1.16 mm^{-1} for the 1SG/1C/1SG specimen. The strain at fragmentation, ϵ_C, calculated by this equation was validated using the FE model discussed in Section 5.2 and the relative difference found to be less than 0.2%. Therefore, this simple equation can be applied to find the strength of the carbon/epoxy layer at the second knee point. At the start of the plateau the difference in the overall measured extension and strain in the carbon ply is negligible. However,
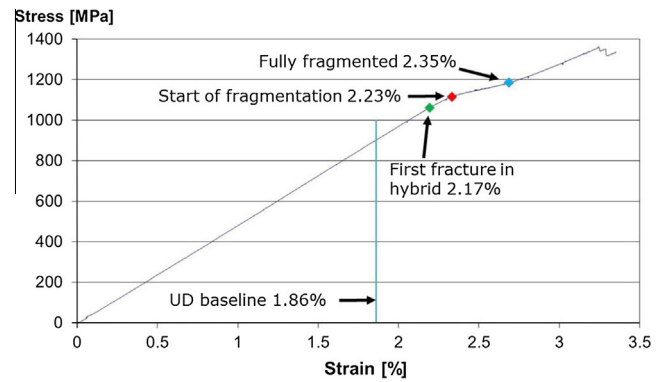

Fig. 8. A typical stress–strain curve of the 1SG/1C/1SG hybrid specimen with carbon failure strains highlighted at different stages. Labelled values are averages calculated from all tested specimens rather than measured directly on the specimen shown.

as the carbon layer fragmentation gradually introduces gaps between the ends of the fragments, the average strain in the carbon layer increasingly deviates from the overall extension.

The average overall stress at the end of the plateau in the experimental results determined from the intersection of lines fitted to sections of the test graphs before and after the knee point is equal to 1202 MPa for the 1SG/1C/1SG sample. Putting this value into Eq. (1), with the moduli and thicknesses from Table 2, the value of strain in the carbon layer is found to be 2.381% for the single ply case. The overall stress of 1162 MPa for the 1SG/2C/1SG specimens gives a strain of 2.131% at fragmentation saturation at the end of the plateau. The effect of thermal residual strains after fragmentation saturation is less than in the laminate without any fracture of the carbon layer since fragmentation allows the stresses to relax via interfacial deformation. So the compressive thermal strains quoted in Table 4 are the upper bound, but to be conservative, they are subtracted from the values found from Eq. (2). As a result, the failure strain of the 1SG/1C/1SG laminate at fragmentation saturation is at least 2.352% and the failure strain of the 1SG/2C/1SG is at least 2.108%.

It is worth mentioning that the thermal residual strains at fragmentation saturation are location dependent and may vary between zero and the values in Table 4 along each fragment. The maximum strains are compared in Table 8 with the results presented earlier in Table 6. The strains are more than 5% higher than the values at the start of the plateau. This can be considered as a further type of hybrid effect over and above what is presented in Table 6, as it is possible to go beyond the early failures and reach the strains of the stronger parts of the material, exploiting a greater proportion of the carbon strength distribution in these thin-ply hybrid configurations.

Fig. 8 summarises the overall results for the 1SG/1C/1SG specimens, showing the increasing strains in the carbon layer as the failure process and fragmentation progresses. A typical stress–strain response is plotted, and the strains in the carbon layer at the differ-

ent stages are labelled on the plot. These values are based on the average measured strains for different specimens including corrections for thermal stresses and so do not correspond exactly to the points on the graph. The final value at the end of fragmentation is calculated from Eq. (2), representing the maximum value of the varying strain along the length of the carbon fragments at the point of saturation. It should be noted that this is lower than the measured overall strain on the outer surface of the specimen.

6. Conclusions

Baseline failure strains of carbon/epoxy composites can be significantly underestimated in conventional unidirectional tests, leading to overestimation of hybrid effects. A specimen with carbon plies sandwiched between glass plies has been found to give consistent gauge length failures away from stress concentrations at the grips, and can be used to determine reference failure strains.

The magnitude of the hybrid effect depends on the ply thickness. For the carbon/S-glass–epoxy there is a hybrid effect of up to 20% at the first knee on the stress–strain curve when the carbon is only 29 µm thick, but there is no significant effect for plies over 80 µm thick. The hybrid effect can be separated into different parts: an effect on initiation of failure, due to constraint at the fibre level, and another effect due to delay in establishing stable fragmentation as a result of constraint at the ply level. There is a further increase in strain during fragmentation as increasing stress is required to form successive critical clusters in the carbon layer. Models have been presented which are able to illustrate all of these mechanisms, and give reasonable quantitative results for the hybrid effects.

These results illustrate how the strain in the carbon layers increases as the failure progresses from first ply fracture to establishment of progressive ply fragmentation to saturation of the fragmentation process. They demonstrate that different values for the hybrid effect are possible depending on how the point of failure is defined. At initiation, delay in failure is possible because of the constraining effect at the fibre level on the development of critical clusters of fibre breaks due to the limited number of fibres through the thickness of the ply. During fragmentation there is a constraint at the ply level that limits the development of further clusters of fibre breaks, allowing greater advantage to be taken of the variable strength of the ply. In both cases the hybrid effect occurs because of the possibility of making use of a greater proportion of the distribution of the strength of the carbon fibres.

Acknowledgements

References

[1] Hayashi T. On the improvement of mechanical properties of composites by hybrid composition. In: Proc 8th int reinforced plastics conference. p. 49–52.

[2] Swolfs Y, Gorbatikh L, Verpoest I. Fibre hybridisation in polymer composites: a review. Composites Part A 2014;67:181–200.

[3] Phillips LN. The hybrid effect – does it exist? Composites 1976;7(1):7–8.

[4] Bunsell AR, Harris B. Hybrid carbon and glass fibre composites. Composites 1974;4:157–64.

[5] Aveston J, Sillwood JM. Synergistic fiber strengthening in hybrid composites. J Mater Sci 1976;11(10):1877–83.

[6] Zweben C. Tensile strength of hybrid composites. J Mater Sci 1977;12(7):1325–37.

[7] Xing J, Hsiao GC, Chou TW. A dynamic explanation of the hybrid effect. J Compos Mater 1981;15(Sep):443–61.

[8] Fukuda H, Chou TW. Stress concentrations in a hybrid composite sheet. J Appl Mech-Trans ASME 1983;50(4A):845–8.

[9] Manders PW. The strength of mixed fibre composites PhD thesis. Surrey, United Kingdom: University of Surrey; 1979.

[10] De Baere I, Van Paepegem W, Degrieck J. On the design of end tabs for quasi-static and fatigue testing of fibre-reinforced composites. Polym Compos 2009;30:381–90.

[11] Wisnom MR, Maheri MR. Tensile strength of unidirectional carbon fibre-epoxy from tapered specimens. In: 2nd European Conf. on composites testing and standardisation. Hamburg; September 1994. p. 239–47.

[12] Khan B, Potter K, Wisnom MR. Suppression of delamination at ply drops in tapered composites by ply chamfering. J Compos Mater 2006;40:157–74.

[13] Czél G, Jalalvand M, Wisnom MR. Hybrid specimens eliminating stress concentrations in tensile and compressive testing of unidirectional composites. Composites Part A [submitted for publication].

[14] Jalalvand M, Czel G, Wisnom MR. Numerical modelling of the damage modes in UD thin carbon/ glass hybrid laminates. Compos Sci Technol 2014;94:39–47.

[15] Fuller JD. Pseudo-ductility of thin ply angle-ply laminates PhD thesis. University of Bristol; 2015.

[16] Czél G, Wisnom MR. Demonstration of pseudo-ductility in high performance glass–epoxy composites by hybridisation with thin-ply carbon prepreg. Composites Part A 2013;52:23–30.

[17] Czél G, Jalalvand M, Wisnom MR. Demonstration of pseudo-ductility in unidirectional hybrid composites made of discontinuous carbon/epoxy and continuous glass/epoxy plies. Composites Part A 2015;72:75–84. http://dx.doi.org/10.1016/j.compositesa.2015.01.019.

[18] Czél G, Jalalvand M, Wisnom MR. Design and characterisation of advanced pseudo-ductile unidirectional thin-ply carbon/epoxy–glass/epoxy hybrid composites. Compos Struct 2016;143:362–70.

[19] Gigliotti M, Wisnom MR, Potter KD. Development of curvature during the cure of AS4/8552 [0/90] unsymmetric composite plates. Compos Sci Technol 2003;63:187–97.

[20] Wisnom MR. Size effects in the testing of fibre-composite materials. Compos Sci Technol 1999;59:1937–57.

[21] Wisnom MR, Khan B, Hallett SR. Size effects in unnotched tensile strength of unidirectional and quasi-isotropic carbon/epoxy composites. Compos Struct 2008;84:21–8.

[22] Swolfs Y, McMeeking RM, Gorbatikh L, Verpoest I. The effect of fibre dispersion on initial failure strain and cluster development in unidirectional carbon/glass hybrid composites. Composites Part A 2015;69:279–87.

[23] Swolfs Y, McMeeking RM, Verpoest I, Gorbatikh L. Matrix cracks around fibre breaks and their effect on stress redistribution and failure development in unidirectional composites. Compos Sci Technol 2015;108:16–22.

[24] Swolfs Y, Verpoest I, Gorbatikh L. Issues in strength models for unidirectional fibre-reinforced composites. Compos Sci Technol 2015;114:42–9.

[25] Swolfs Y, Gorbatikh L, Romanov V, Orlova S, Lomov SV, Verpoest I. Stress concentrations in an impregnated fibre bundle with random fibre packing. Compos Sci Technol 2013;74:113–20.

[26] Rosen BW. Tensile failure of fibrous composites. AIAA J 1964;2:1985–91.

[27] Swolfs Y, Gorbatikh L, Verpoest I. Stress concentrations in hybrid unidirectional fibre-reinforced composites with random fibre packings. Compos Sci Technol 2013;85:10–6.

[28] Kelly A, Zweben C. Comprehensive composite materials. Elsevier; 2000.

[29] Naito K, Yang J-M, Kagawa Y. Tensile properties of high strength polyacrylonitrile (PAN)-based and high modulus pitch-based hybrid carbon fibers-reinforced epoxy matrix composite. J Mater Sci 2012;47(6):2743–51.

[30] Naito K, Yang JM, Tanaka Y, Kagawa Y. The effect of gauge length on tensile strength and Weibull modulus of polyacrylonitrile (PAN)- and pitch-based carbon fibers. J Mater Sci 2012;47(2):632–42.

[31] Thomason JL. On the application of Weibull analysis to experimentally determined single fibre strength distributions. Compos Sci Technol 2013;77:74–80.

[32] Xing J, Hsiao GC, Chou TW. A dynamic explanation of the hybrid effect. J Compos Mater 1981;15(SEP):443–61.

[33] Jalalvand M, Hosseini-Toudeshky H, Mohammadi B. Numerical modeling of diffuse transverse cracks and induced delamination using cohesive elements. Proc Inst Mech Eng, Part C: J Mech Eng Sci 2013;227(7):1392–405.

[34] Jalalvand M, Czél G, Wisnom MR. Damage analysis of pseudo-ductile thin-ply UD hybrid composites – a new analytical method. Composites Part A 2015;69:83–93.